J. Fluid Mech. (2015), *vol.* 779, *pp.* 544–555. © Cambridge University Press 2015
doi:10.1017/jfm.2015.428

Power-law exponent in the transition period of decay in grid turbulence

L. Djenidi[1,†], Md. Kamruzzaman[1] and R. A. Antonia[1]

[1]Discipline of Mechanical Engineering, School of Engineering, University of Newcastle, Newcastle, 2308 NSW, Australia

(Received 19 March 2015; revised 15 July 2015; accepted 21 July 2015; first published online 18 August 2015)

Hot-wire measurements are carried out in grid-generated turbulence at moderate to low Taylor microscale Reynolds number Re_λ to assess the appropriateness of the commonly used power-law decay for the mean turbulent kinetic energy (e.g. $k \sim x^n$, with $n \leqslant -1$). It is found that in the region outside the initial and final periods of decay, which we designate a transition region, a power law with a constant exponent n cannot describe adequately the decay of turbulence from its initial to final stages. One is forced to use a family of power laws of the form x^{n_i}, where n_i is a different constant over a portion i of the decay time during the decay period. Accordingly, it is currently not possible to determine whether any grid-generated turbulence reported in the literature decays according to Saffman or Batchelor because the reported data fall in the transition period where n differs from its initial and final values. It is suggested that a power law of the form $k \sim x^{n_{init}+m(x)}$, where $m(x)$ is a continuous function of x, could be used to describe the decay from the initial period to the final stage. The present results, which corroborate the numerical simulations of decaying homogeneous isotropic turbulence of Orlandi & Antonia (*J. Turbul.*, vol. 5, 2004, doi:10.1088/1468-5248/5/1/009) and Meldi & Sagaut (*J. Turbul.*, vol. 14, 2013, pp. 24–53), show that the values of n reported in the literature, and which fall in the transition region, have been mistakenly assigned to the initial stage of decay.

Key words: homogeneous turbulence, isotropic turbulence, turbulent flows

1. Introduction

Since the pioneering work of Taylor (1935), homogeneous isotropic turbulence (HIT) has been extensively studied in grid turbulence, which consists in passing a uniform flow through a grid made of vertical and horizontal bars placed normal to the main flow. Accordingly, over almost 80 years, grid turbulence has been used for testing various theories of HIT including, for example, self-similarity laws, Kolmogorov's similarities (Kolmogorov (1941*a*,*b*), hereafter denoted K41) and the decay law of the turbulent kinetic energy. One of the main difficulties with grid turbulence is to generate turbulence at high Reynolds numbers (e.g. Re_λ, the Taylor microscale Reynolds number; $Re_\lambda = u'\lambda/\nu$, where u' is the r.m.s. velocity, λ the Taylor microscale and ν the kinematic viscosity of the fluid). Only a few experiments

† Email address for correspondence: lyazid.djenidi@newcastle.edu.au

were successful in achieving relatively high Re_λ by using so-called active grids (e.g. Mydlarski & Warhaft 1996, 1998; Larssen & Davenport 2001; Kang, Chester & Meneveau 2003). Recently, in a very interesting experiment, Sinhuber, Bodenschatz & Bewley (2015) carried out measurements in passive grid turbulence with very high Reynolds number in the range $5 \leqslant x/M \leqslant 40$ by using air and pressurized sulphur hexafluoride (x is the distance downstream of the grid and M the grid mesh size). Note though that the results need to be analysed with care because, as shown by Isaza, Salazar & Warhaft (2014) (see also Lavoie 2006), turbulence in the region $x/M \leqslant 10$–15 has an 'anomalous' behaviour similar to that seen in fractal-grid turbulence, i.e. a larger decay power-law exponent and a turbulent kinetic energy dissipation coefficient that varies like Re_λ^{-1} (Valente & Vassilicos 2011) (it should be mentioned that the latter variation is also observed in the 3D periodic turbulence of Goto & Vassilicos (2015)). In the near-field region downstream of the grid, the streamwise inhomogeneity may not be sufficiently weak to be neglected. Also the variation of Re_λ with x is strong enough so that it cannot be ignored. The reason for working with turbulence at high Reynolds number is to test HIT theories when there is a large separation between the large and small scales, i.e. when an inertial range exists and is represented by the $5/3$ law in the Kolmogorov-normalized velocity spectrum or the $2/3$ law in the second-order velocity structure function (K41). While the experimental implementation of high Re_λ grid turbulence is challenging, the realizability of very low Re_λ grid turbulence (i.e. final stage of decaying turbulence (Batchelor & Townsend 1948)) is equally challenging. In this latter case, the intensity of the background turbulence level is of the order of or greater than the turbulence generated by the grid, thus making the measurements of the decay practically impossible. There is also the practical issue associated with the fact that low Re_λ grid turbulence requires long distances downstream of the grid for the turbulence to become homogeneous in planes perpendicular to the mean flow. Thus, an experimental study of the final period of decaying turbulence is extremely difficult, if not impossible. There have been a few experimental investigations of the final period (e.g. Tan & Ling 1963; Ling & Huang 1970; Tavoularis, Bennett & Corrsin 1978), but the results are still inconclusive for the reason cited above.

The difficulties encountered in achieving decaying grid turbulence with either very high or very low Reynolds number mean that the issue of the decay of the turbulent kinetic energy, k, is yet to be resolved. The lack of ideal flow conditions (e.g. very high or very low Re_λ) forces researchers to investigate the decay of turbulence in grid turbulence with low to moderate Reynolds number, e.g. Re_λ ranging from about 30 to 80. It is commonly believed that turbulence decays as a power law of the form $k \sim x^n$, where x is the downstream distance behind the grid and n is a negative constant. So far, the theoretical predictions show that turbulence may decay according to Batchelor (1949) or Saffman (1967). Note though that these predictions are valid only at very high and very low Re_λ. The first measurements in grid turbulence appeared to show that $n = -1$ (e.g. Batchelor & Townsend 1947). But it is now well accepted that $n \leqslant -1$, at least in grid turbulence generated in laboratories where Re_λ is neither very high nor very small. Under these conditions, the decay of turbulence is yet to be resolved, as illustrated by the various values of n reported in the literature. For example, in recent times, Krogstad & Davidson (2010), who carried out measurements in grid turbulence with several grid geometries, argued that the turbulence behind a grid decays according to Saffman ($n = -1.2$, Saffman 1967). Hearst & Lavoie (2014) reported values of n of about -1.37 and -1.39 in turbulence behind a fractal grid (for various values of n in decaying turbulence behind classical grids see Mohamed & LaRue (1990) and Lavoie, Djenidi & Antonia (2007)).

Recent numerical simulations (Meldi & Sagaut 2013) based on the eddy-damped quasi-normal Markovian (EDQNM) model of decaying HIT showed that the turbulence is in a transition period (from the initial to the final stages) when Re_λ ranges from approximately 1 to 100. The EDQNM results imply that, if one assumes that the turbulence decays according to a power law, then the power exponent n cannot be constant. Interestingly, this transition regime covers the range of Re_λ at which experiments in grid turbulence are carried out. Since it is well accepted that $|n_{init}| \leqslant |n_{final}|$, where $|n_{init}|$ and $|n_{final}|$ are the decay exponents at the initial and final stages of the decay, respectively, then n must vary from its initial period value to its final period value (as shown by Meldi & Sagaut 2013). In an earlier numerical study of decaying HIT, Orlandi & Antonia (2004), who compared results based on EDQNM, pseudospectral DNS and finite differences DNS, also reported a variation of n for $4 \leqslant Re_\lambda \leqslant 2000$.

The non-constancy of n would suggest that one needs to use a family of power laws of the form t^{n_i}, where n_i is a different constant over a portion i of the decay time during this transition period. If one then accepts that a series of power laws with different decay exponents is required to describe the decay of turbulence in the transition period, one is then forced to conclude that it is not possible to assess whether the turbulence decays according to Saffman ($n_{init} = -1.2$, $n_{final} = -1.5$; Saffman 1967), Batchelor ($n_{init} = -10/7$, $n_{final} = -2.5$; Batchelor 1949) or any other possible type of decay from a single grid turbulence experiment if either the initial or the final stage of the decay is not part of the decay range covered by the measurements. Bekritskaya & Pavel'ev (1983) analysed the data of Batchelor (1948) and Gad-el-Hak & Corrsin (1974) and suggested that the decay could be approximated by a power law provided that the exponent increases with decreasing Reynolds number.

The present work focuses on the decay of a grid-generated turbulence when Re_λ varies from about 6 to 100. The aim of the study is to assess the appropriateness of a power-law decay of the form $k \sim x^n$ and the behaviour of the exponent n.

2. Experimental set-up and measurement technique

The experiment is carried out in an open-circuit wind tunnel that was also used by Lavoie *et al.* (2007) and Lee *et al.* (2012). The air flow is driven by a centrifugal blower which is controlled by a variable-cycle (0–1500 r.p.m.) power supply. The blower is supported by dampers and connected to the tunnel by a flexible joint to minimize possible vibrations. At the inlet to a plenum chamber, an air filter (594 mm × 594 mm × 96 mm) captures particles from the flow and a honeycomb ($l/d \simeq 4.3$) removes residual swirl. A wire screen with an open area ratio of 63 % and a smooth 9:1 primary contraction at the outlet of the plenum chamber improve the uniformity of the flow. A secondary (1.36:1) short contraction is mounted at a fixed location downstream of the turbulence generator, which corresponds to $x/M = 6.2$, 19.2 and 54 for the LSQ43, SSQ43 and WMD36 grids (see below), respectively. This contraction is used to improve global isotropy (Comte-Bellot & Corrsin 1966) (more information on the secondary contraction can be found in Lavoie *et al.* (2007)). Because the velocity of the flow is accelerated when fluid flows through the secondary contraction an 'equivalent' time is defined as follows (Comte-Bellot & Corrsin 1966; Mohamed & LaRue 1990; Lavoie *et al.* 2007):

$$t = \int_0^x \frac{\mathrm{d}s}{\langle U(s) \rangle} \tag{2.1}$$

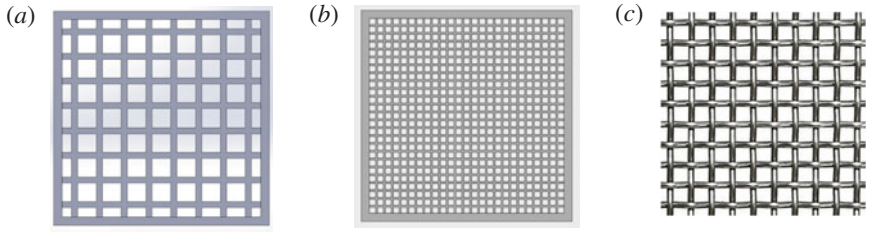

FIGURE 1. The geometry of the two different perforated grids (LSQ43 and SSQ43) and the woven mesh grid (WMG36).

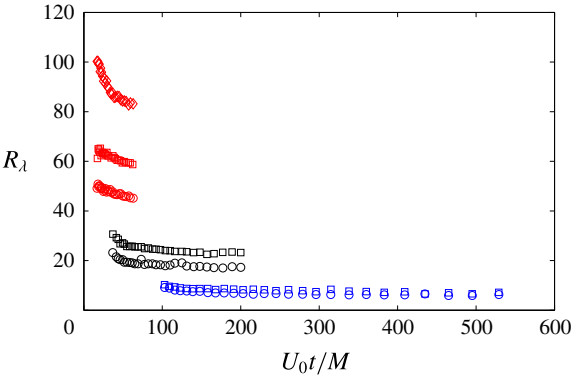

FIGURE 2. (Colour online) Streamwise variation of Re_λ for the grids used in the study. Red open symbols: ◇, □, ○ LSQ43 grid ($Re_M = 37\,500$, 17 900 and 12 950); black open symbols: □, ○ SSQ43 grid ($Re_M = 5800$ and 4170); blue open symbols: □, ○ WMG36 grid ($Re_M = 1474$ and 1200).

where $\langle U(s)\rangle$ is measured at the centreline of the working section. The angular brackets denote time averaging.

Three grids are used to generate turbulence in the wind tunnel (figure 1). The first (LSQ43) is a flat plate perforated with large square holes yielding a mesh of size $M = 43.75$ mm and solidity, σ, of about 43 %. The second, also made from a flat plate perforated with small square holes (SSQ43), has a mesh size $M = 14.15$ mm and the same solidity as the LSQ43 grid. The mesh size ratio between LSQ43 and SSQ43 is 3:1. The third is a woven mesh grid (WMG36) with $\sigma = 36\,\%$ and $M = 5$ mm. The effect of the grid mesh Reynolds number $Re_M = U_0M/\nu$ on the decay of turbulence is investigated at several different speeds. The use of these three grids and different values of U_0, the incoming velocity, yielded values of Re_λ in the range 6–100.

The streamwise variation of Re_λ for the three grids is presented in figure 2. Notice how the rate of decrease of Re_λ reduces as Re_M decreases. This makes the measurements at small Reynolds numbers quite difficult as a very large distance is required for Re_λ to change significantly.

The measurements of the velocity fluctuations u and v in the longitudinal and lateral directions, respectively, were carried out using hot-wire anemometry; both single and X wires were used. The wires (diameter $d \approx 2.5$ μm and length $l = 200d$) were etched from a coil of Wollaston (platinum) and were operated with in-house constant-temperature anemometers (hereafter, CTA) at overheat ratio of 1.5. The

output signals from CTA circuits were amplified, offset and low-pass filtered at a cutoff frequency (f_c) close to the Kolmogorov frequency $f_K = U_0/2\pi\eta$, where $\eta\,(= \nu^{3/4}\langle\epsilon\rangle^{-1/4})$ is the Kolmogorov length scale; $\langle\epsilon\rangle$ is the mean dissipation rate of the turbulent kinetic energy. The sampling frequency f_s was at least $2f_c$. The hot-wire signals were digitized into a PC using a ± 10 V and 16 bit AD converter. Measurements were conducted at several distances downstream from the grid. The ratio η/l varied from about 0.26 to about 3.6 across all measurement sets.

3. Results

3.1. Re_λ dependence of the power-law decay

The decay of the mean turbulent kinetic energy downstream of a grid is commonly represented by a power law:

$$\langle q^2\rangle = A(x - x_0)^n \tag{3.1}$$

where $\langle q^2\rangle = \langle u^2\rangle + \langle v^2\rangle + \langle w^2\rangle$ is twice the turbulent kinetic energy, $x\,(= tU_0/M$, t is the time) is a distance downstream of the grid, x_0 is a virtual origin and $n \leqslant -1$; A, x_0 and n are to be determined empirically. Note that, strictly, the distance x as used in (3.1) is not the actual distance downstream of the grid but an equivalent one as it accounts for the acceleration of the flow through the short contraction (i.e. t is given by (2.1)). Since $v^2 = w^2$ in the turbulence generated by each grid, we have $\langle q^2\rangle = \langle u^2\rangle + 2\langle v^2\rangle$, which eliminates the necessity to measure the third velocity component. For the single-wire measurements, we used $\langle q^2\rangle = \langle u^2\rangle(1 + 2/r_{uv})$ with $r_{uv} = \langle u^2\rangle/\langle v^2\rangle$ estimated from the X-wire measurements. A, x_0 and n are assumed to be constant in (3.1). Yet, one expects that $|n|$ should increase to reach its final value n_{final} when Re_λ decreases. In grid turbulence, Re_λ decreases with increasing x, as shown in figure 2, and thus one can expect that $|n|$ increases with x. However, if the rate of change in Re_λ over some distance x is small enough (see figure 2), one may assume n to be constant to a first approximation; this is the usual approach reported in the literature. Figure 2 indicates that, while such an approximation seems valid for SSQ43 and WMG36 over a relatively long distance, it is not as evident for LSQ43 because of the relatively short distance. Nevertheless, we follow the common practice of assuming that the variation in Re_λ for the LSQ43 grid is small enough in the region $U_0t/M \geqslant 25$ to ignore. Thus, for each set of measurements with the three grids, n will be assumed to be independent of x and (3.1) will hold, as illustrated in figure 3, which shows, in a log–log representation, the variation of both $\langle q^2\rangle$ and $\langle\epsilon\rangle$ with the distance $(x - x_0)/M$. The figure shows that $\langle q^2\rangle$ follows a straight line relatively well for each grid, supporting the law (3.1) over the range of x considered. Since the transport equation for $\langle q^2\rangle$ in grid turbulence is

$$\langle\epsilon\rangle = -\frac{U_0}{2}\frac{\partial\langle q^2\rangle}{\partial x}, \tag{3.2}$$

then using (3.1) leads to $\langle\epsilon\rangle \sim (x - x_0)^{n-1}$. It is important to stress that, strictly, (3.2) holds when the production of the turbulent and viscous diffusions of $\langle q^2\rangle$ is zero, which is the case in grid turbulence when x is at least larger than $20M$–$25M$. Djenidi & Antonia (2014) showed that $\langle\epsilon\rangle = (\nu/2)\langle(\partial u_i/\partial x_j) + (\partial u_j/\partial x_i)\rangle$, with all terms included, satisfies (3.2) when $x/M \geqslant 25$ behind a grid made of floating flat square elements and with a solidity of about 25 %. They also found that (3.2) cannot be used to obtain $\langle\epsilon\rangle$ when $x/M \leqslant 25$ (see also Lavoie 2006). The power-law decay

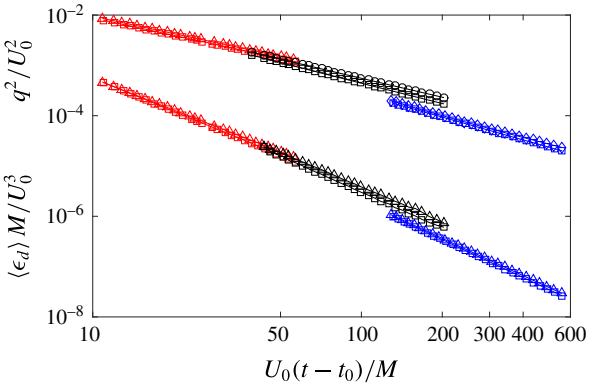

FIGURE 3. (Colour online) Decay of $\langle q^2\rangle$ and $\langle\epsilon\rangle$ for different grids and Re_M. Open red symbols: LSQ43, □: $Re_M = 17900$, △: $Re_M = 12950$. Open black symbols: SSQ43, □: $Re_M = 5800$, △: $Re_M = 4170$. Open blue symbols: WMG36, □: $Re_M = 2000$, △: $Re_M = 1474$.

Grids	U_0 (m s^{-1})	U_0t_0/M	r_{uv}	$-n$	Re_λ	Re_M	η/M	L/M
LSQ43	12.8	6.1	na	1.13 ± 0.03	100−84	37 500	(0.003−0.006)	(0.35−0.57)
LSQ43	6.4	6.6	0.97	1.14 ± 0.02	65−58	17 900	(0.004−0.010)	(0.35−0.58)
LSQ43	4.6	5.8	0.95	1.15 ± 0.04	50−45	12 950	(0.005−0.010)	(0.36−0.59)
SSQ43	6.4	−2.0	0.85	1.26 ± 0.02	30−23	5800	(0.03−0.06)	(0.57−0.90)
SSQ43	4.6	−2.0	0.84	1.36 ± 0.02	23−17	4170	(0.02−0.05)	(0.59−1.00)
WMG36	6.4	−26.0	na	1.46 ± 0.03	12−9	2000	(0.10−0.25)	(0.90−1.70)
WMG36	4.6	−28.0	1.1	1.50 ± 0.02	10−7	1474	(0.12−0.30)	(0.94−1.78)
WMG36	3.6	−28.0	na	1.52 ± 0.03	9−6	1200	(0.15−0.36)	(0.99−1.87)

TABLE 1. Decay exponent n for LSQ43, SSQ43 and WMG36.

of $\langle\epsilon\rangle$ is supported by the data in figure 3. The slope of the straight lines, which gives the value of $|n|$, increases as Re_M (or equivalently Re_λ) decreases, confirming that the magnitude of n increases with a decreasing Re_λ. It is interesting that the value of $\langle\epsilon\rangle$ inferred from (3.2) is equal to the isotropic value $\langle\epsilon_{iso}\rangle$, which Djenidi & Antonia (2014) showed is equal to the actual value of $\langle\epsilon\rangle$ for $x/M \geqslant 10$.

The determination of n is conditioned by x_0. It is then critical that x_0 is obtained as accurately and unambiguously as possible. In this study, it was estimated by using a trial-and-error method adopted by Comte-Bellot & Corrsin (1966) and later Lavoie *et al.* (2007). Assuming the decay laws (3.1) and (3.2), we have $\lambda^2 = 10\nu(q^2/\langle\epsilon\rangle) = -(10\nu/U_0n)((tU_0/M_0) - (t_0U_0/M))$. Different values of tU_0/M $(= x_0)$ were tried until $\lambda^2/MU_0(t - x_0)$ exhibited the longest plateau when plotted against $U_0(t - t_0)/M$. This is illustrated in figure 4 for SSQ43 at $Re_M = 4710$. Lavoie *et al.* (2007) showed that the uncertainty in x_0 is about ± 1, which results in a ± 0.03 variation in the estimate of n.

Table 1 contains values of U_0, x_0, n, the ratio r_{uv}, Re_λ, Re_M, η/M and L/M. Interestingly, the values of x_0 and r_{uv} for a given grid appear to be independent of Re_M. Of interest are the values of η/M and L/M across the various set of measurements. The maximum value of L/M is about 1.9, which suggests that the lateral dimensions of the tunnel are large enough to neglect any effect they may have on the decay of turbulence. Figure 5(*a*) shows the variation of n as function of Re_λ.

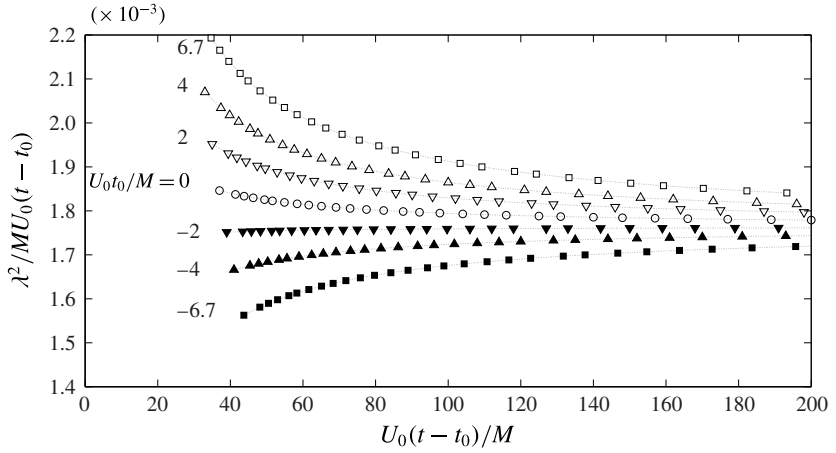

FIGURE 4. Examples of plots used for estimating the virtual origin. Ratio $\lambda^2/MU_0(t-t_0)$ for SSQ43 and $U_0 = 4.6$ m s^{-1}. The curve exhibiting the longest plateau corresponds to U_0t_0/M used in the power law (3.1).

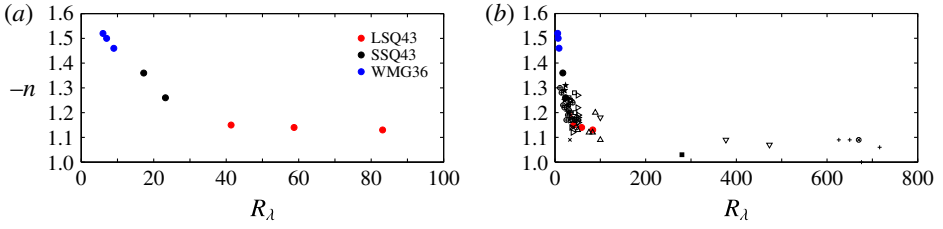

FIGURE 5. (Colour online) Decay exponent n as function of Re_λ. (*a*) Present three grids. (*b*) Selection of data from the literature. See table 2 for the symbols and their references.

We also show in figure 5(*b*) various values of n extracted from several studies cited in table 2. The trend of the present data (figure 5*a*) is consistent with that seen in figure 5(*b*), i.e. the value of $-n$ increases when Re_λ decreases. When Re_λ becomes large, n tends to approach a constant. It is not clear whether the scatter observed for n at large Re_λ is due to measurement uncertainties or reflects an actual effect of the initial conditions. These measurements were obtained in active decaying grid turbulence (see table 2 for the references).

Figure 5 highlights the need to exercise caution when interpreting the results of decaying grid turbulence in the context of determining whether it follows the Saffman ($n = -1.2$; Saffman 1967) or Batchelor ($n = -10/7$; Batchelor 1948) decay laws at low Re_λ. In particular, when the Reynolds number is below about 100, one cannot conclude, solely on the basis of the value of n, whether the turbulence decays according to Saffman (1967) or Batchelor (1948) because n has departed from its value at high Reynolds number, and Re_λ is not small enough for n to have reached its 'final period' value. The present results do not agree with the results of Ling & Huang (1970), who argue that $n = -2$ when $Re_\lambda \leqslant 30$.

The present variation of the decay exponent with Re_λ is compared (figure 6) with that from the numerical simulations of Orlandi & Antonia (2004) and Meldi & Sagaut (2013). The data of Orlandi & Antonia (2004) correspond to Batchelor decaying

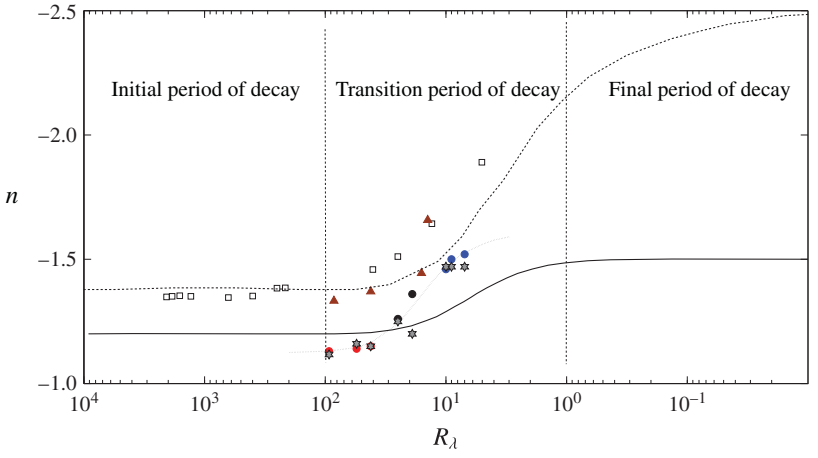

FIGURE 6. (Colour online) Variation of n as function of Re_λ. Solid circles, same as in figure 5; stars, present data using (3.3) (the thin dash-dotted line through the symbols is used only as a visual guide); solid triangles, EDQNM (Orlandi & Antonia 2004); □, pseudospectral (Orlandi & Antonia 2004); lines, EDQNM (Meldi & Sagaut 2013) with $n_{init} = -10/7$ (dashed) or $n_{init} = -1.2$ (solid). The transition regime is only tentatively delimited by the vertical lines. This range corresponds to that in which the majority of the data for n, as inferred from decaying turbulence behind passive grids, has been reported.

turbulence, while those of Meldi & Sagaut (2013) correspond to both Batchelor and Saffman decaying turbulence. Meldi & Sagaut (2013) showed that different curves $n = f(Re_\lambda)$ are obtained with different initial values of n_{init}. Although the EDQNM curves deviate from the experimental data, both the experiments and simulations indicate unambiguously that n varies in the transition period, thus revealing that the decay of turbulence cannot strictly follow a unique power law in this transition period. Nevertheless, one may consider using a family of power laws of the form x^{n_i}, where n_i is a different constant over a portion i of the decay time during this transition period or region. A possible practical alternative that one can infer from figure 6 is to use a power law of the form $\langle q^2 \rangle \sim x^{n_{init}+m(x)}$, where the continuous function $m(x)$ is such that $n_{final} - n_{init} \leqslant m(x) \leqslant 0$. This latter form could be used to describe the entire decay (i.e. initial, transient and final stages). Since most of the grid turbulence measurements are carried out in the transition region, it is not surprising that a rather large range of values of n has been reported in the literature and mistakenly assigned to the initial period of decay. Interestingly, the experimental values of $-n$ at the higher Re_λ fall below those of both Saffman and Batchelor. While no definite conclusion can be drawn from figure 6 on the actual type of decay, this result does not support the argument that grid turbulence, at least when generated by the present grids, is likely to follow Saffman (Krogstad & Davidson 2010), although it is closer to Saffman than Batchelor. Further, the data in figure 5(*b*) suggest that the decay of turbulence behind active grids follows neither Saffman nor Batchelor, as indicated by the values of n at large Re_λ.

Recently, Djenidi & Antonia (2015) used a self-preservation (SP) analysis on the scale-by-scale energy budget equation for decaying HIT and developed an expression for n with an explicit dependence on Re_l:

$$n = -1 + 2(t - t_0)\frac{1}{Re_l}\frac{\mathrm{d}Re_l}{\mathrm{d}t}. \tag{3.3}$$

Reference	Grid	Re_{λ_u}	Symbol
Batchelor & Townsend (1947)	Passive	21−29	⋆
Batchelor & Townsend (1947)	Active	28−30	⋆
Comte-Bellot & Corrsin (1971)	*Sq*34*	47	⊙
Huang & Leonard (1994)	Simulation	10−50	⊕
Kang *et al.* (2003)	Active	625−716	+
Kistler & Vrebalovich (1966)	Rd33.5	670	⊗
Lavoie (2006)	Sq35	43−44	□
Lavoie (2006)	Rd35	30	□
Lavoie (2006)	Sq35	43−44	□
Mydlarski & Warhaft (1996)	Passive	50−100	▽
Mydlarski & Warhaft (1996)	Active	267−473	▽
Lee *et al.* (2012)	Rd44	37	×
Lee *et al.* (2012)	Rd44W	33	×
Lee *et al.* (2012)	Rd35	25	×
Lee *et al.* (2012)	Sq35	40	×
Schedvin, Stegen & Gibson (1974)	Sq30	280	■
Zhou & Antonia (2000)	Sq35	50−100	△
Zhou & Antonia (2000)	Sq35	50−55	▷
Zhou & Antonia (2000)	Sq35	34−43	▷
Present data (2014)	LSQ43	41−100	
	SSQ43	17−29	
	WMG36	6−12	

TABLE 2. Reference table for the decay exponent. Symbols are used in figure 5(*b*). The data were compiled by Lee *et al.* (2013).

where Re_l is a Reynolds number based on a set of velocity and length scales conforming with SP. Expression (3.3) is valid strictly when SP is satisfied at all scales of motion. If one assumes that SP is approximately satisfied in decaying grid turbulence, i.e. Re_λ varies weakly downstream of the grid, then one can expect (3.3) with Re_λ replacing Re_l to be approximately valid. This appears to be confirmed in figure 6, where the values of n calculated with (3.3) are reported. There is relatively good agreement between these latter values and those of n inferred from the power-law decay.

Note that care must be taken when measuring n when a power-law decay is assumed. One must ensure that Re_λ decreases weakly in the region considered. This is not the case in the near-grid region, as highlighted in figure 2. This is most evident for a fractal-grid turbulence (Valente & Vassilicos 2011; Hearst & Lavoie 2014) where the near-grid region is larger than for conventional grid turbulence. Despite this shortcoming, Valente & Vassilicos (2011) and Hearst & Lavoie (2014) measured n and found values of about -2.5 and -2.79, respectively, in the near-grid region. Associated with a rapid decay of turbulence in the near grid, one must also consider the effect of the lateral inhomogeneity of the flow caused by the individual wakes generated by the grid elements. Corrsin (1963) proposed at least three criteria that must be satisfied for ensuring homogeneity in grid turbulence (grid made of horizontal and vertical bars): (i) large grid porosity, (ii) large $L = M$ (L is the height/diameter of the wind tunnel) and (iii) measurements should be taken at least $40M$ downstream of the grid (see also Grant & Nisbet 1957). As mentioned in the introduction, recently Sinhuber *et al.* (2015) carried out measurements in a (conventional) passive grid

turbulence with very high Reynolds number ($10^4 \leqslant Re_M \leqslant 5 \times 10^6$; unfortunately no value of Re_λ is provided in their paper). They measured $n = -1.18$, and argued that the turbulence decays according to Saffman. However, while the Reynolds number is very high, the range of x/M over which they measured n falls within the region where turbulence is not homogeneous. Further, the results of Sinhuber *et al.* (2015) contrast with those of Isaza *et al.* (2014), who showed that the turbulence in the region $5 \leqslant x/M \leqslant 15$ is not homogeneous and $n = -1.9$, while $n = -1.34$ for $15 \leqslant x/M \leqslant 70$. They also showed that turbulence in the first range (referred to as the near-field) displays an anomalous behaviour similar to that observed in fractal-grid turbulence. Nevertheless, it is noteworthy to point out that Sinhuber *et al.* (2015) made a compilation of values of n as a function of Re_M from previous studies in decaying HIT. The trend shown by the data is in good agreement with the present results. However, the authors did not identify the transitional period and attributed the variation of n with Re_M to changes in initial and boundary conditions between experiments.

Finally, comments are warranted on the nature of the initial and transition periods of decay in HIT. The initial period is associated with a high Re_λ and an approximately constant n followed by the transition period where n varies. In grid turbulence, the hypothesis of HIT can only be valid when the flow becomes homogeneous in a plane perpendicular to the main flow and very weakly inhomogeneous along the main flow, which, according to Corrsin (1963), is well observed when $x/M \geqslant 40$. It is thus important not to associate the decay of turbulence in the region $x/M \leqslant 40$ with the initial period, even though Re_λ can be large; or at least one must ensure that turbulence is homogeneous in a plane perpendicular to the main flow in that region. On the other hand, so far, the decay in passive grid turbulence observed in the literature for $x/M \geqslant 40$ where the values of n fall within the range obtained here is consistent with the transition period observed in this study.

4. Conclusion

A grid-generated turbulence at moderate to low Re_λ was investigated with the aim of ascertaining whether the commonly used power-law decay of the turbulent kinetic energy, k, is appropriate. Several grid geometries were used to allow Re_λ to vary from about 6 to 100, a range that covers most of the Reynolds numbers obtained in passive grid turbulence reported in the literature. It is shown that the decay of turbulence does not strictly follow a power law of the form $k \sim x^n$ with n constant. The results, supported by the numerical data of decaying HIT (Orlandi & Antonia 2004; Meldi & Sagaut 2013) and the experimental results (see Sinhuber *et al.* (2015) for a compilation of values of n in various experiments and simulations of decaying HIT), suggest that, on an empirical ground at least, one may consider using a family of power laws of the form x^{n_i}, where n_i is a different constant over a portion i of the decay time during this transition period, with $|n_i|$ increasing as Re_λ decreases, and $n_{final} \leqslant n_i \leqslant n_{init}$. A possible practical alternative for describing the entire decay is $\langle q^2 \rangle \sim x^{n_{init}+m(x)}$, where $n_{final} - n_{init} \leqslant m(x) \leqslant 0$.

The present study sheds light on the lack of consensus in the literature on the value of n for what is presumed to be the initial period of decay for grid turbulence. It also underlines the current impossibility of differentiating between the Batchelor and Saffman predictions for the value of n in the initial period. The range -1.4 to -1.1 for n reported in the literature indicates that the measurements have almost certainly been carried out in what should more appropriately be designated as the transition period of decay, at least for passive decaying grid turbulence.

To address properly the question of the decay of turbulence behind a grid, one is required to perform measurements in a very long wind tunnel so the variation of Re_λ downstream of the grid is significant enough to lead to a non-negligible variation in n, if a solution in the form of a power law is sought. The range of x/M to consider for such a study should correspond to the range where turbulence is homogeneous in the lateral directions and weakly inhomogeneous in the streamwise direction. This range is beyond the near-grid region of classical grid turbulence that Hearst & Lavoie (2014) and Isaza *et al.* (2014) identified with the 'anomalous' behaviour range.

The present results (e.g. figure 6) suggest that, ideally, the Taylor microscale Reynolds number should vary from about 0.1 to about 300. Sinhuber *et al.* (2015) showed that a very high Re_M can be achieved with conventional passive grids in the region $x/M \leqslant 30$. However, these high Re_M measurements need to be extended in the region $x/M \geqslant 40$ and over a long distance so both the initial and the transition periods of the decay can be observed in grid turbulence. The final period of decay can be achieved over a long distance downstream of the grid, but the background turbulence prevents any reliable measurements.

Acknowledgement

The financial support of the Australian Research Council is gratefully acknowledged.

REFERENCES

BATCHELOR, G. K. & TOWNSEND, A. A. 1947 Decay of vorticity in isotropic turbulence. *Proc. R. Soc. Lond.* A **190**, 534–550.

BATCHELOR, G. K. & TOWNSEND, A. A. 1948 Decay of turbulence in the final period. *Proc. R. Soc. Lond.* A **194**, 527–543.

BATCHELOR, G. K. 1948 Energy decay and self-preserving correlation functions in isotropic turbulence. *Quart. Appl. Math.* **6**, 97–116.

BATCHELOR, G. K. 1949 The role of big eddies in homogeneous turbulence. *Proc. R. Soc. Lond.* A **195**, 513–532.

BEKRITSKAYA, S. I. & PAVEL'EV, A. A. 1974 On the power law of decay of grid turbulence. *Izv. Akad. Nauk SSSR Mekh. Zhidk. Gaza* **4**, 170–172; (Engl. Trans.).

COMTE-BELLOT, G. & CORRSIN, S. 1966 The use of a contraction to improve the isotopy of grid-generated turbulence. *J. Fluid Mech.* **25**, 657–682.

COMTE-BELLOT, G. & CORRSIN, S. 1971 Simple Eulerian time correlation of full- and narrow-band velocity signals in grid-generated, 'isotropic' turbulence. *J. Fluid Mech.* **48**, 273–337.

CORRSIN, S. 1963 *Turbulence: Experimental Methods*. vol. 8. Springer.

DJENIDI, L. & ANTONIA, R. A. 2014 Transport equation for the mean transport energy dissipation rate in low-R_λ grid turbulence. *J. Fluid Mech.* **747**, 288–315.

DJENIDI, L. & ANTONIA, R. A. 2015 A general self-preservation analysis for decaying homogeneous isotropic turbulence. *J. Fluid Mech.* **773**, 345–365.

GAD-EL-HAK, M. & CORRSIN, S. 1974 Measurements of the nearly isotropic turbulence behind a uniform jet grid. *J. Fluid Mech.* **62**, 115–143.

GOTO, S. & VASSILOCOS, J. C. 2015 Energy dissipation and flux laws for unsteady turbulence. *Phys. Lett.* A **379** (16–17), 1144–1148.

GRANT, H. L. & NISBET, I. C. T 1957 The inhomogeneity of grid turbulence. *J. Fluid Mech.* **2**, 263–272.

HEARST, R. J. & LAVOIE, P. 2014 Decay of turbulence generated by a square-fractal-element grid. *J. Fluid Mech.* **741**, 567–584.

HUANG, M.-J. & LEONARD, A. 1994 Power-law decay of homogeneous turbulence at low Reynolds numbers. *Phys. Fluids* **480**, 129–160.

ISAZA, J. C., SALAZAR, R. & WARHAFT, Z. 2014 On grid-generated turbulence in the near- and far field regions. *J. Fluid Mech.* **753**, 402–426.

KANG, H. S., CHESTER, S. & MENEVEAU, C. 2003 Decaying turbulence in an active-grid-generated flow and comparisons with large eddy simulation. *J. Fluid Mech.* **480**, 129–160.

KISTLER, A. L. & VREBALOVICH, T. 1966 Grid turbulence at large Reynolds numbers. *J. Fluid Mech.* **26**, 37–47.

KOLMOGOROV, A. 1941*a* Dissipation of energy in the locally isotropic turbulence. *Dokl. Akad. Nauk SSSR* **32**, 16–18.

KOLMOGOROV, A. 1941*b* On the degeneration (decay) of isotropic turbulence in an incompressible viscous fluid. *Dokl. Akad. Nauk SSSR* **31**, 538–540.

KROGSTAD, P.-Å. & DAVIDSON, P. A. 2010 Is grid turbulence Saffman turbulence? *J. Fluid Mech.* **642**, 373–394.

LARSSEN, J. V. & DAVENPORT, W. J. 2001 On the generation of large-scale homogeneous turbulence. *Exp. Fluids* **50**, 1207–1223.

LAVOIE, P. 2006 Effects of initial conditions in decaying grid turbulence. PhD thesis, University of Newcastle, Australia.

LAVOIE, P., DJENIDI, L. & ANTONIA, R. A. 2007 Effects of initial conditions in decaying turbulence generated by passive grids. *J. Fluid Mech.* **585**, 395–420.

LEE, S. K., BENAISSA, A., DJENIDI, L., LAVOIE, P. & ANTONIA, R. A. 2012 Scaling range of velocity and passive scalar spectra in grid turbulence. *Phys. Fluids* **24**, 075101.

LEE, S. K., DJENIDI, L., ANTONIA, R. A. & DANAILA, L. 2013 On the destruction coefficients for slightly heated decaying grid turbulence. *Intl J. Heat Fluid Flow* **43**, 129–136.

LING, S. C. & HUANG, T. T. 1970 Decay of weak turbulence. *Phys. Fluids* **13**, 2912–2914.

MELDI, M. & SAGAUT, P. 2013 Further insights into self-similarity and self-preservation in freely decaying isotropic turbulence. *J. Turbul.* **14**, 24–53.

MOHAMED, M. S. & LARUE, J. C. 1990 The decay power law in grid-generated turbulence. *J. Fluid Mech.* **219**, 195–214.

MYDLARSKI, L. & WARHAFT, Z. 1996 On the onset of high-Reynolds number grid-generated wind tunnel turbulence. *J. Fluid Mech.* **320**, 331–368.

MYDLARSKI, L. & WARHAFT, Z. 1998 Passive scalar statistics in high-Peclet-number grid turbulence. *J. Fluid Mech.* **358**, 135–175.

ORLANDI, P. & ANTONIA, R. A. 2004 Dependence of a passive scalar in decaying isotropic turbulence on the Reynolds and Schmidt number using the EDQNM model. *J. Turbul.* **5**, doi:10.1088/1468-5248/5/1/009.

SAFFMAN, P. G. 1967 Note on decay of homogeneous turbulence. *Phys. Fluids* **10**, 1349.

SCHEDVIN, J., STEGEN, G. R. & GIBSON, C. H. 1974 Universal similarity at high grid Reynolds numbers. *J. Fluid Mech.* **65**, 561–579.

SINHUBER, M., BODENSCHATZ, E. & BEWLEY, G. P. 2015 Decay of turbulence at high Reynolds numbers. *Phys. Rev. Lett.* **114**, 034501.

TAN, H. S. & LING, S. C. 1963 Final stage decay of grid produced turbulence. *Phys. Fluids* **6**, 1693–1699.

TAVOULARIS, S., BENNETT, J. C. & CORRSIN, S. 1978 Velocity-derivative skewness in small Reynolds number, nearly isotropic turbulence. *J. Fluid Mech.* **88**, 63–69.

TOWNSEND, A. A. 1956 *The Structure of Turbulent Shear Flow*. Cambridge University Press.

TAYLOR, G. I. 1935 Statistical theory of turbulence. *Proc. R. Soc. Lond.* A **151**, 412–478.

VALENTE, P. C. & VASSILICOS, J. C. 2011 The decay of turbulence generated by a class of multiscale grids. *J. Fluid Mech.* **687**, 300–430.

ZHOU, T. & ANTONIA, R. A. 2000 Reynolds number dependence of the small-scale structure of grid turbulence. *J. Fluid Mech.* **406**, 81–107.